Bulletin of Geophysics and Oceanography Vol. 65, n. 4, pp. 701-714; December 2024
DOI 10.4430/bgo00454

Hydrocarbon reservoir parameter estimation using a fuzzy Gaussian based SVR method

N. Moosavi[1], M. Bagheri[2] and M. Nabi-Bidhendi[2]

[1] *Department of Earth Sciences, Science and Research Branch, Islamic Azad University, Tehran, Iran*
[2] *Department of Earth Physics, Institute of Geophysics, University of Tehran, Tehran, Iran*

(Received: 29 March 2023; accepted: 12 February 2024; published online: 24 May 2024)

ABSTRACT Measuring effective porosity helps in evaluating the capacity of rock to contain fluid. In this paper, we estimated porosity in one of the oil fields in southern Iran. For this purpose, we used a well-known method of Support Vector Machine due to its ability to produce models with less risk of overfitting and a good generalisation capacity. Considering that used data are always contaminated with noise, we combined this method with a fuzzy system using membership functions. Different types of membership functions are available and they are chosen on the basis of data distribution. Membership functions add importance and prioritise data points. Each data point is evaluated with respect to the whole data and receives a coefficient between 0 and 1. Data points with coefficient closer to zero have a lower priority in the algorithm and data points with coefficient closer to one have a higher priority and are more important in the algorithm. To compare the fuzzy system effect, the coefficient of determination is calculated for the model including noise. A lower priority is attributed to random noise in data with respect to normal data. The result shows that using fuzzy systems notably improves the robustness of a model in the presence of noise.

Key words: porosity, Support Vector Machine, Fuzzy Support Vector Machine, noise, coefficient of determination.

1. Introduction

Petrophysical parameters play an important role in the evaluation of hydrocarbon reservoirs. Over the last decades, the application of artificial intelligence (AI) methods has become popular in assessing reservoirs. Machine Learning (ML) is a subdivision of AI that gives computers the ability to learn, tries to find a pattern among data sets and to address such patterns for all the data.

ML has been widely used by various authors over recent years (Rezaee *et al.*, 2008; Al-Anazi and Gates, 2012; Teixeira and Secchi, 2019; Mohamed *et al.*, 2020), to evaluate reservoir parameters. Bagheri and Riahi (2015) used facies analysis and seismic data for reservoir modelling, while Bagheri *et al.* (2013) and Saputro *et al.* (2016) used Artificial Neural Network (ANN) to estimate porosity. Rafik and Kamel (2016) predicted porosity by means of both nonparametric regression and an ANN method. Sinaga *et al.* (2019) predicted porosity by integrating an ANN and seismic attributes. Huang *et al.* (2021) used Support Vector Regression (SVR) based on particle swarm

optimisation (PSO) to estimate the recovery rate of reservoirs in complicated geological areas.

The Support Vector Machine (SVM), introduced at first by Vapnik (1995), is used for both Support Vector Classification (SVC) and SVR. The SVM is based on structural risk minimisation (SRM). In algorithms functioning on the basis of SRMs, empirical errors and Vapnik-Chervonenkis (C) confidence intervals are both minimised (Vapnik, 1982, 1995). Compared to models based on empirical risk minimisation (ERM), models based on SRM overcome the problem of overfitting and have better generalisation properties (Al Anazi and Gates 2012). In ERM algorithms, the training data errors are minimised and the model depends highly on training data distribution.

The SVM classification algorithm calculates a line (or hyperplane in the case of higher dimensions) that maintains the maximum distance between two classes. For this reason, the line with the maximum distance relates to the SVM concept (Fig. 1a). For the purpose of regression, the SVM concerns data points overlaid by a tube with radius of epsilon. Some of the data points are located inside the tube, some are on the tube while others are outside it. The SVR algorithm aims to estimate a function inside and alongside of the tube, with a maximum distance from the tube (Fig. 1b).

In the SVM, the distance of the data points outside the tube is penalised by the use of the epsilon-insensitive loss function (Fig. 2). Three main factors affect the accuracy and precision of the SVM model in regression: the tube radius, *C* parameter, and kernel function. The *C* parameter is a factor that deals with the complexity of the model and the amount of error attributed to data points outside the tube. Kernel functions, instead, enable distributing data points in a space of higher dimension, where the classification or regression problem can be solved more easily.

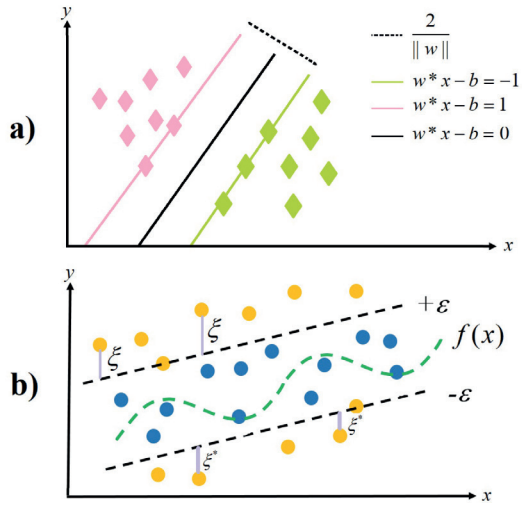

Fig. 1 - Application of a SVM for classification (a) and regression (b).

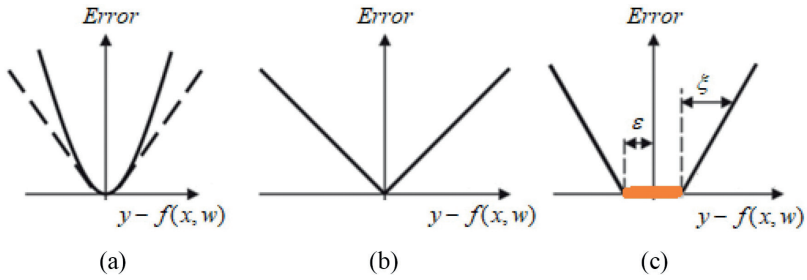

Fig. 2 - Illustration of three loss functions: a) the Huber loss function (black dotted line), b) the L1 norm or Laplace, and c) the ε-insensitive loss function.

In this paper, the SVM is used for the purpose of regression. The reason for using the ML method in this paper is that porosity should be estimated for a hydrocarbon zone and, obviously, the best method to find reservoir properties is to use core data. However, core data are not always available and are usually expensive. In addition, estimating properties from well log data is condition-based and not always accurate. Therefore, to overcome these problems, the SVM was utilised as it is suitable for the volume of data of this study and for the advantages it brings compared to other methods (it is SRM-based instead of ERM-based). Accordingly, we modelled a function to predict porosity for the area, so as to use it to estimate reservoir porosity for areas with limited core data availability.

Various works have been done so far on SVMs for modelling hydrocarbon reservoirs. For example, Basak *et al.* (2007) compared the SVM with the ANN to verify how these two different approaches reach a global minimum. Al Anazi and Gates (2012) showed how SVR is capable of predicting reservoir parameters with a small sample size of training data. Gholami *et al.* (2012) compared the SVM with the regression neural network (RNN) for permeability prediction and found that a SVM is more accurate and faster than an RNN. Bagheri and Rezaei (2019) estimated permeability using radial basis functions. Moosavi *et al.* (2023a) predicted permeability using electro-facies logs on input data to be used in a fuzzy SVR algorithm to estimate permeability, and, in fact, Moosavi *et al.* (2023b) predicted water saturation using the fuzzy SVR method. Yin *et al.* (2020) used the SVM and PSO to model reservoirs with highly dispersed physical properties. Moosavi *et al.* (2022) compared the fuzzy *C* means with the fuzzy SVR to estimate porosity from noisy data.

In this paper, to estimate a better porosity model for the whole area, the effect of three very important parameters, which required proper selecting to notably improve the model, were investigated. The authors worked on SVR parameter tuning and selection (Villmann *et al.*, 2015; Wang and Xu, 2017). The way in which these parameters affect the model, whether by improving or deteriorating it, is evaluated in this paper.

Ultimately, worthy of mention is the fact that noise is an unseparated part of data. Data processing removes only a part of noise as some noise still remains, even after processing. By using membership functions, a fuzzy system was applied on data to overcome the noise problem. The robustness of the algorithm was checked before and after applying the fuzzy system against noise. The results prove the superiority of the fuzzy SVM compared to the SVM.

2. Methodology

2.1. Support Vector Machine (SVM)

The SVM can be used for solving both SVC and SVR problems. To understand SVC, we can imagine two label classes as shown in Fig. 1. There are, certainly, many lines that can separate these two groups from each other. The SVM classifies two groups of data based on the maximum distance from the line separating the data into two groups (Gunn, 1998). The data points of each class closest to the other class are called support vectors (Smola and Scholkopf, 1998), and are indicated in pink and green diamonds on the green and pink lines in Fig. 1a. In the figure, the black line ($w \times x - b = 0$) is the SVM classifier that keeps the greatest distance between class 1 (pink diamonds) and class 2 (green diamonds). The pink and green lines representing the passing support vectors of each group are given by ($w \times x - b = 1$) and ($w \times x - b = -1$), respectively, where w is the normal vector (the black line). The distance between the support vectors is equal to

$\frac{2}{\|w\|}$ and becomes maximum when $\|w\|$ is minimum (Vapnik, 1995). A data set, with training data x_n with N observations and response observed values y_n, is described as follows:

$$(x_1, y_1),(x_2, y_2),...,(x_L, y_L) \qquad x \in R^n. \tag{1}$$

Minimising $\|w\|$ leads to the minimisation of $w^T w$:

$$\|w\| = \sqrt{(w^T w)} = \sqrt{w_1^2 + w_2^2 + ... + w_n^2}. \tag{2}$$

To minimise $w^T w$, the following equation must be solved:

$$L(w,b,\alpha) = \frac{1}{2} w^T w - \sum_{i=1}^{l} \alpha_i \left\{ y_i \left[w^T x_i + b \right] - 1 \right\} \tag{3}$$

where a_i are the Lagrangian coefficients. The purpose is to find the saddle point of (w_0, b_0, a_0). After solving the problem, the line or hyperplane can be obtained as below (Suykens *et al.*, 2002):

$$D(x) = \sum_{i=1}^{l} w_{0i} x_i + b_0 = \sum_{i=1}^{l} y_i \alpha_i x_i^T x + b_0. \tag{4}$$

Concerning the solving of regression problems with SVM algorithms, at this point, a tube with radius of ε located on the data points should be taken into consideration. Some of the data are located inside or on the tube, while the rest are located outside the tube (Fig. 1b). Data points inside the tube receive no penalty (blue circles in Fig. 1b), but data outside the tube receive a penalty, which is proportional to their distance from the tube (orange circles out of the tube in Fig. 1b). The farther from the tube, the larger the penalty received. The SVM tries to find a function, which minimises the penalty of data points outside of the ε-tube and also to maximise the distance between the function and the ε-tube (Fig. 1b, where ξ, $\xi^*$are the penalty of data points and also the distance between the black and green dotted lines to be maximised).

To apply penalty to slack variables (ξ), various loss functions can be used. These loss functions are displayed in Fig. 2. The Huber loss function is indicated in Fig. 2a with a black dotted line. Fig. 2b shows the Laplace or L1 norm, which is less sensitive to outliers compared to Fig. 2a. Fig. 2c shows the *E*-insensitive loss function, which promotes sparsity in a greater manner than the two other functions (Rustam *et al.*, 2019). The *E*-insensitive loss function assigns no penalty to data points, which are inside the ε-tube (the orange area in Fig. 2c), but data points located out of the *E*-tube receive a penalty value.

The SVM implementation in this study applies the Vapnik *E*-insensitivity loss function to penalise the data points outside the tube (Vapnik, 1995). The formula below describes how slack variables receive penalty:

$$(y - f(x))_\varepsilon = \begin{cases} 0 & if\ |y - f(x)| \le \varepsilon \\ |y - f(x)| - \varepsilon & Otherwise \end{cases}. \tag{5}$$

If the predicted value is within the tube the loss is zero. Conversely, if the predicted value is outside the tube, the loss is given by the difference between the predicted value and the tube radius.

Consequently, the optimisation problem for SVR is the following:

$$Min_{w,b}\frac{1}{2}||w||^2 + C\sum_{i=1}^{N}(\xi_i + \xi_i^*) \tag{6}$$

subjected to:

$$\begin{aligned}&\forall n: y_n - (Xn'w + b) \le \varepsilon + \xi_n\\ &\forall n: (Xn'w + b) - y_n \le \varepsilon + \xi_n^*\\ &\forall n: \xi_n^* \ge 0\\ &\forall n: \xi_n \ge 0\end{aligned} \tag{7}$$

where *C* creates a balance between model complexity and slack variables associated to data falling outside the tube, which must be minimised (empirical risk). Lagrangian multipliers α_i and α_i^* are obtained by solving the dual optimisation problem, as here following:

maximise:

$$-\frac{1}{2}\sum_{i,j=1}^{n}(\alpha_i - \alpha_i^*)(\alpha_j - \alpha_j^*)<X_i.X_j> - \epsilon\sum_{i=1}^{n}(\alpha_i + \alpha_i^*) + \sum_{i=1}^{n} y_i(\alpha_i - \alpha_i^*) \tag{8}$$

subject to:

$$\sum_{i=1}^{n}(\alpha_i - \alpha_i^*) = 0 \quad and \quad \alpha_i, \alpha_i^* \in [o, c] \tag{9}$$

where α_i and α_i^* are positive Lagrange multipliers. Consequently *f*(*x*) and *w* for the SVR model is calculated with:

$$w = \sum_{i=1}^{N}(a_i - a_i^*)X \tag{10}$$

$$f(x) = \sum_{i=1}^{n}(\alpha_i - \alpha_i^*) < X_i X > + b. \tag{11}$$

Kernel functions are the third parameters affecting SVR models. A kernel helps in the application of linear classifiers to non-linear problems by mapping non-linear data to a higher dimensional space. In addition, in case of regression problems, a kernel helps to find a function that better fits the data by mapping the data in higher dimensional space (Gunn, 1998). Fig. 3 shows how data are transferred to higher dimensions to be linearly classified with the help of kernels.

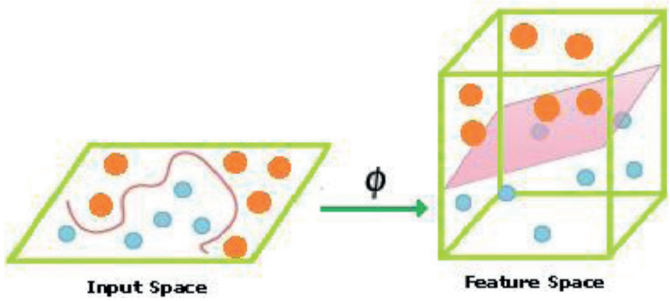

Fig. 3 - Illustration of data transformed into higher dimensions using the kernel trick.

2.2. Fuzzy Support Vector Regression (SVR)

Measured core data and well logs used as the input of SVR models contain noise that can affect the output of the SVR model. To find a solution for this problem, SVR is modified to fuzzy SVR, which can control the amount of noise in data much better than SVR (Bishop, 2006). Fuzzy SVR applies membership functions on data points so that every data point receives a degree of membership. In this way, every data point has a contribution on the output model (Rustam *et al.,* 2019). In this case, noise and outliers receive a lower degree of membership compared to other data points. For this reason, reducing the effect of noise on the model may be helpful.

Fuzzy membership degree is indicated with S_i for data points and (1 - S_i) for noisy data. The fuzzy concept was first introduced by Zadeh (1965). Following his paper, we transferred data points to a [0, 1] interval to normalise them. We, then, found the normalised data average. Data points identified by numbers bigger than the average are called X_+ and are class 1 with label +1 (y_i = +1), and data points labelled by numbers smaller than the average are called X_-, and are class 2 with label -1 (y_i = -1) (Lin and Wang, 2002). S_i is defined as follows:

$$S_i = \begin{cases} 1 - |X_+ - X_i|/(r_+ - \delta) \; where \; y_i = 1 \\ 1 - |X_- - X_i|/(r_- + \delta) \; where \; y_i = -1 \end{cases} \tag{12}$$

r_+ and r_- are as follows:

$$r_+ = \max|X_+ - X_i| \; where \; y_i = 1 \tag{13}$$

$$r_- = \max|X_- - X_i| \; where \; y_i = -1. \tag{14}$$

Therefore, to modify SVR to fuzzy SVR, each data point is multiplied by S_i and the new data set becomes the new input for the SVR algorithm.

3. Application

3.1. Geology of the region

The mentioned methodology was tested on real data field. The Belal oil field is located in the central Persian Gulf, 80 km SE of Lavan Island and 40 km SE of the South Pars oil field, adjacent to the Qatar-Iran border (Fig. 4). Three well sets were drilled in 1972 and 1973 in this area,

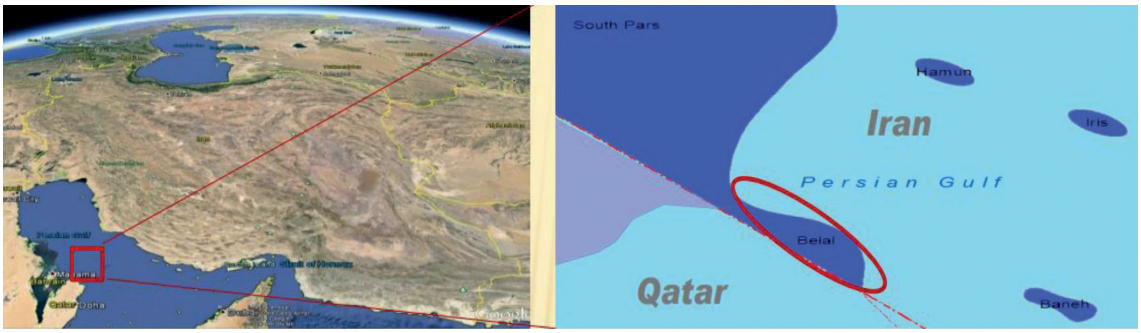

Fig. 4 - Map of the Belal oil field located in the Persian Gulf. Hamun, Iris, South Pars, and Baneh are oil and gas fields in the region.

leading to the discovery of this oil field with three main hydrocarbon intervals. The Arab-Hith formation is the main reservoir in this area, the upper Dalan-Kangan formation has the second priority and Sarvak-Darian has the third rank in the Belal oil field (Esrafili-Dizaji and Rahimpour-Bonab, 2013). The Arab-Hith formation in this area mainly consists of dolomite, anhydrite, and limestone. For this study, the authors were granted access to two well sets and their associated core data.

3.2. Input data for the SVR algorithm

In this paper, four well logs were chosen to estimate porosity. The log curves included acoustic sonic log (DT) neutron porosity (NPHI), gamma ray (GR), and bulk density (RHOB). Fig. 5a displays the four logs over the reservoir area. Fig. 5b displays the core porosity, which will be used as output data for the SVR algorithm. The reason for choosing these four well log curves is that they are closely related to porosity, and, as a result, the porosity parameter can be predicted from these logs. Other well logs are less important in calculating porosity, and, if they are chosen as input data, there is no certainty that they will improve the results (Karimian *et al.*, 2013).

4. Discussion and results

To predict porosity, four well logs related to two well sets were used in this study. The authors were also given access to the porosity core data of two well sets to use them for the test and validation operation. The data used in this paper are from two well sets located at different vertical depths. The data of the first well are from shallower depths, while the data of the second are from deeper depths. Data from the first well were used to train the fuzzy SRM predictor. The result was, then, used to predict porosity from the four logs on the second well, and the prediction was compared with the field porosity measurements.

After creating the model, the authors check how the SVR parameters affect the result. For this purpose, different amounts of tube radius ε, C, and kernels are evaluated, consecutively. A small C parameter means that more data points are located on the margin, which is wider. Conversely, a large C parameter means that fewer support vectors are included within the margin, thus the margin is narrower. As a result, as C increases, the model becomes more complex, with a higher risk of overfitting. With an increase of C from 1 to 1,000, the number of support vectors also increases from 53 to 73, as shown in Fig. 6. In this case, a penalty is applied to each data

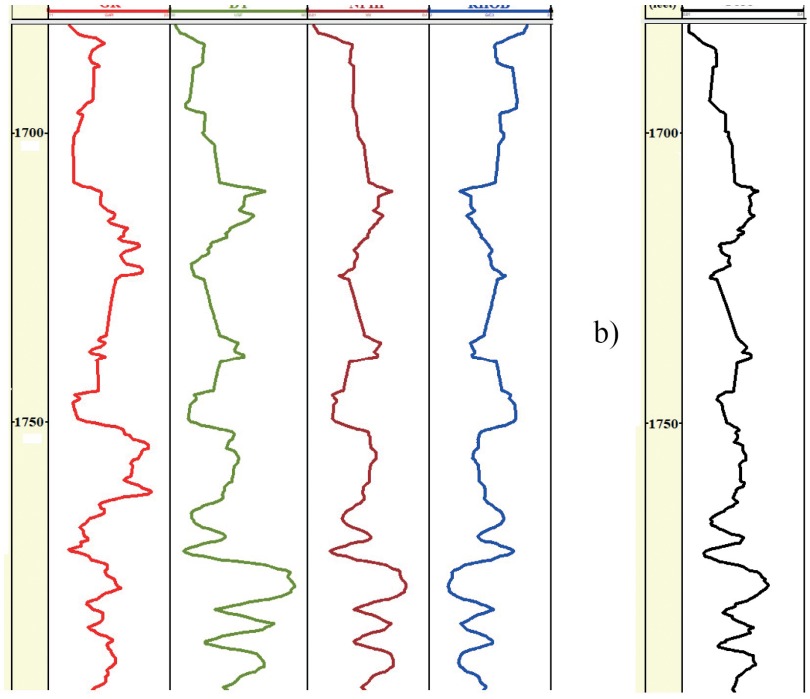

Fig. 5 - Illustration of well logs and core data for porosity estimation used with the SVR algorithm: a) GR (red), DT (green), NPHI (brown) and RHOB (blue); b) core porosity (black) as output data.

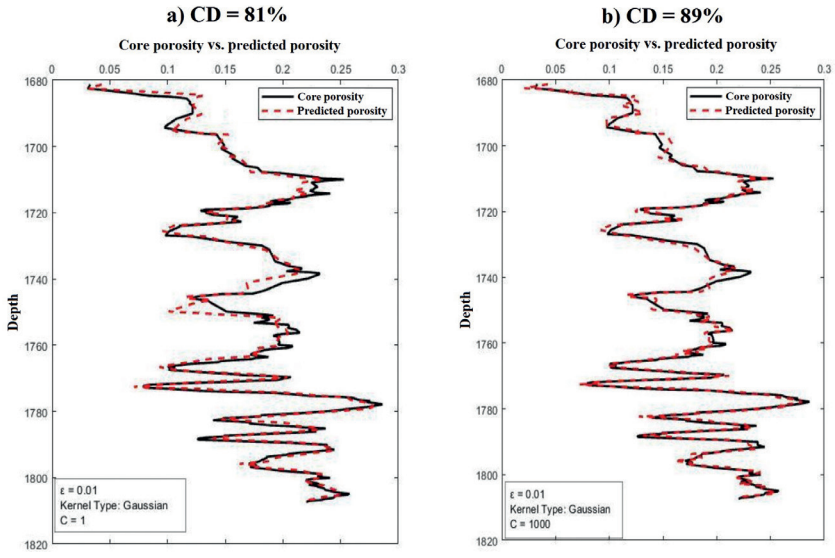

Fig. 6 - Evaluation of the box-constraint effect on the model: a) C = 1, number of accessible support vectors is 53, and coefficient of determination (CD) = 81%; b) C = 1000, number of support vectors has increased to 73. The increase of C has produced a better model (right panel) with CD = 89%.

point located outside the tube. Therefore, as C increases, the accuracy of the model increases between the core data (black line) and the model (red line). However, there is a risk of overfitting that must be considered.

Another factor that determines the tube radius, necessary in finding the regression function, is ε. Data which are located inside the tube receive no penalty and are considered as training data. As Fig. 7 shows, the increase of ε from 0.01 to 0.05 decreases the number of data points falling outside the tube from 127 to 45. In this case, the precision of the model decreases and, consequently, a notable mismatch between core data (black line) and model (red line) is observable.

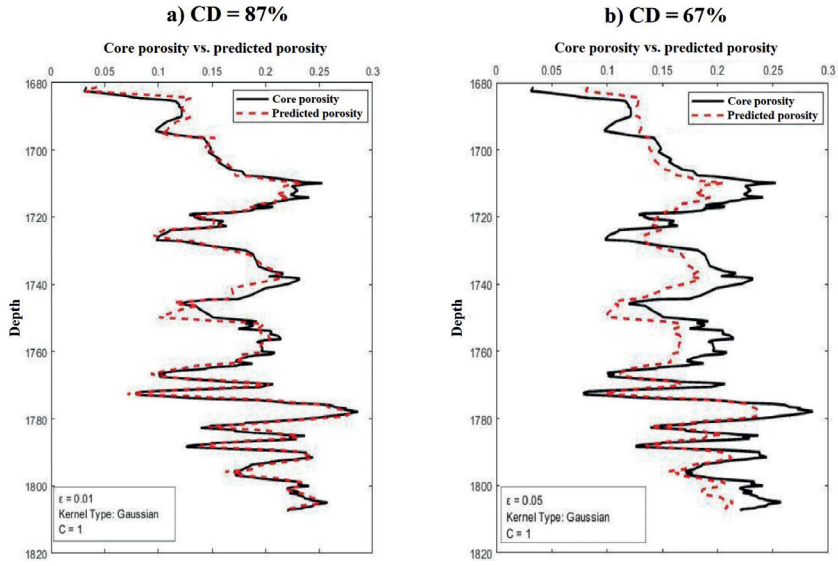

Fig. 7 - Influence of tube radius *e* on the model: a) ε = 0.01, number of accessible support vectors in the model is 127, and *CD* = 87%; b) ε = 0.05, number of support vectors included in the model is 45, and *CD* = 67%. The black curve represents the core porosity and the right curve shows the predicted porosity from SVR.

The last factor is the kernel function. Based on data distribution, an appropriate kernel can increase data separation and fit data more properly. Fig. 8 compares two different kernel functions on the data: a) a Gaussian kernel and b) a polynomial. As the results show, a cubic polynomial kernel with degree 3 fits the data more appropriately when compared to a Gaussian kernel.

The selection of appropriate parameters plays a fundamental role in the accuracy of the model. Three well-known methods are available for choosing the optimal SVR parameters, such as grid search (Hsu *et al.*, 2003), gradient descent (Keerthi *et al.*, 2007), and meta-heuristics algorithms (Blum and Roli, 2003; Talbi, 2009).

In this work, the grid search method, where data are partitioned into two complementary sets, was used. The first set is used for SVR training, and the second for validating SVR prediction. Data training and validation is repeated *K* times. *K* is called fold and can be chosen as an optional

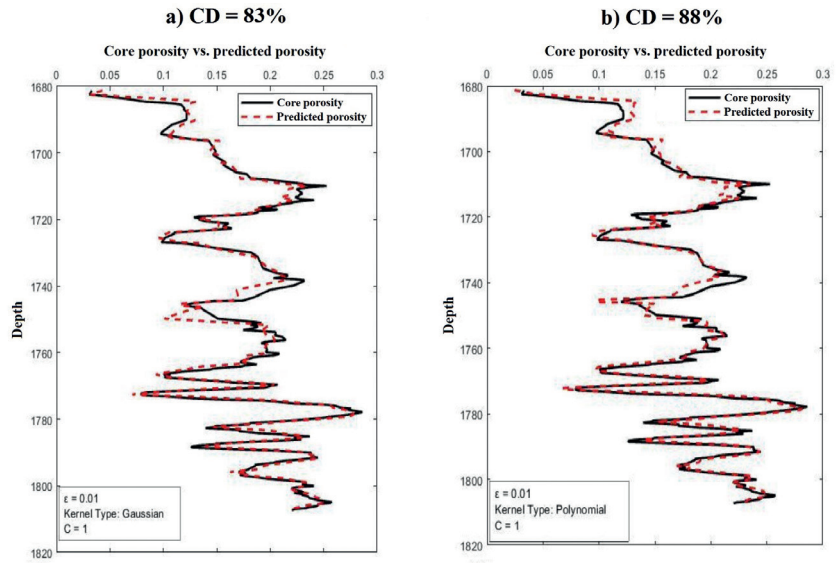

Fig. 8 - Evaluation of two different kernel functions on the model: a) Gaussian type kernel with *CD* = 83%; b) polynomial type kernel (cubic polynomial type, degree 3) with *CD* = 88%. For the current data of this study, the polynomial kernel shows a better result.

number by the user. In each step, the coefficient of determination (*CD*) is calculated for the models obtained from training and validation data. Then, the best data training and test percentage will be obtained in this part. The *CD* is a number between 0 and 1 that measures how well a statistical model predicts the outcome. The *CD* is calculated as expressed below:

$$CD = 1 - \frac{RSS}{TSS} \tag{15}$$

where *RSS* the residual sum of squares and *TSS* the total sum of squares.

The next step consists in individually calculating, for each kernel function, different error statistics such as the *MSE* (mean square error), *MAE* (mean absolute error), and *RMSE* (root mean square error) that measure the accuracy and precision of the model. The *MSE* measures the average of the square errors, that is the average squared difference between the estimated value and the actual value. The *MAE* is measured as the average of the absolute error values. The *RMSE* measures the difference between values predicted by a model and values observed. Formulae for error statistics are reported in Table 1. The use of kernels with less error statistics is recommended. Table 2 displays the results. According to Table 2, for SVR, the *MSE*, *MAE*, and *RMSE*, measured for a coarse Gaussian kernel function, are 0.0014, 0.0299, and 0.0383, respectively. For fuzzy SVR, the quadratic kernel is the most appropriate with *MSE*, *MAE*, and *RMSE* values of 0.00111, 0.212 and 0.033, respectively.

Table 1 - Summary of mathematical expressions.

$MSE = \frac{1}{n}\sum_1^n \ (y_i - \hat{y}_i)^2$	Mean square error
$MAE = \frac{1}{n}\sum_1^n \ \lvert y_i - \hat{y}_i \rvert$	Mean absolute error
$RMSE = \sqrt{\sum_{i=1}^{n} \frac{(y_i - \hat{y}_i)^2}{n}}$	Root mean square error

Table 2 - Data summary for statistical error measurements for different kernel functions.

SVR			
Kernel type	***MSE***	***MAE***	***RMSE***
Linear	0.0014	0.029	0.039446
Quadratic	0.0015	0.029	0.039267
Cubic	0.0018	0.031	0.04265
Medium Gaussian	0.0015	0.0303	0.0397
Coarse Gaussian	0.0014	0.0299	0.0383
Fuzzy SVR			
Kernel type	***MSE***	***MAE***	***RMSE***
Linear	0.00165	0.0235	0.0407
Quadratic	0.00111	0.0212	0.033
Cubic	0.00135	0.0223	0.036
Medium Gaussian	0.0012	0.0229	0.0357
Coarse Gaussian	0.0015	0.027	0.0398

Scatter plots of predicted porosity versus core porosity, using linear kernels, are displayed in Fig. 9 for both SVR and fuzzy SVR. In the second column, the plot shows that data are more concentrated around the 45° line in the fuzzy SVR compared to the SVR model. It can be concluded that better results are obtained from the fuzzy SVR. The *CD* for SVR with core data is 81% while *CD* for fuzzy SVR is 92%.

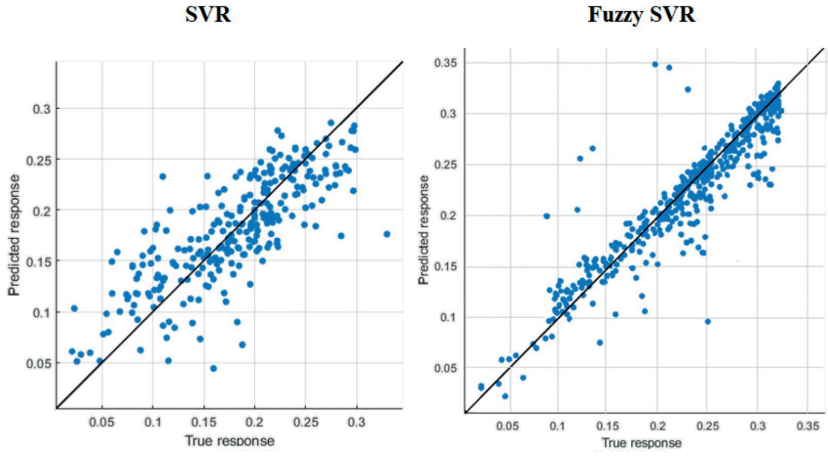

Fig. 9 - Scatter plot of predicted porosity versus core porosity using linear kernels. The *CD* for SVR is 81% and for fuzzy SVR is 92%.

In the final step, to reduce the effect of noise and outliers on data, the membership function is applied on data, so each data point receives a membership degree to be engaged in the fuzzy SVR algorithm. Fig. 10 shows the models obtained from SVR and fuzzy SVR. The results show that the *CD* between core porosity and the SVR model is 79%, while the *CD* between core porosity and fuzzy SVR model is about 90%.

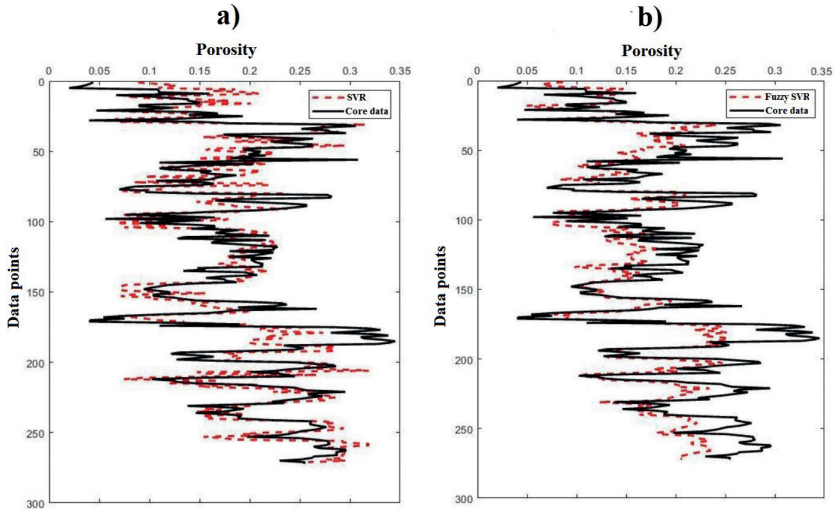

Fig. 10 - Predicted porosity from: a) SVR and b) fuzzy SVR. Core data are indicated with a black line and predicted porosity with a red dotted line.

4.1. Effectiveness of the fuzzy SVR model in the presence of noise in data

To evaluate the effectiveness of the fuzzy SVR model, random noise, equal to 0.5 times the absolute value of the signal amplitude, was added to the training data. Here, the signal is the input data or the well logs. Noise is added to well logs and training data and is not added to the test data or core data. Moosavi *et al.* (2022) explains the amount of random noise that can be added to training data and the amount of random noise that deteriorates SVR or fuzzy SVR. In this paper, the *CD* is calculated for different ranges of random noise using the means of their distribution graphs.

In the next step, both SVR and fuzzy SVR were applied on the noisy data. Fig. 10 shows the results: a) the SVR model (red dotted line) versus core data (black line) and b) the fuzzy SVR model (red dotted line) versus core data (black line). Fig. 11 shows that fuzzy SVR is more robust against noise compared to SVR. The figure also shows how the SVR model has deteriorated in the presence of noise. To understand the numerical difference, the *CD* was calculated for both models and resulted 69% for SVR and 88% for fuzzy SVR. As discussed earlier, the *CD* calculated for SVR and fuzzy SVR without the addition of artificial noise was 79% and 90%, respectively.

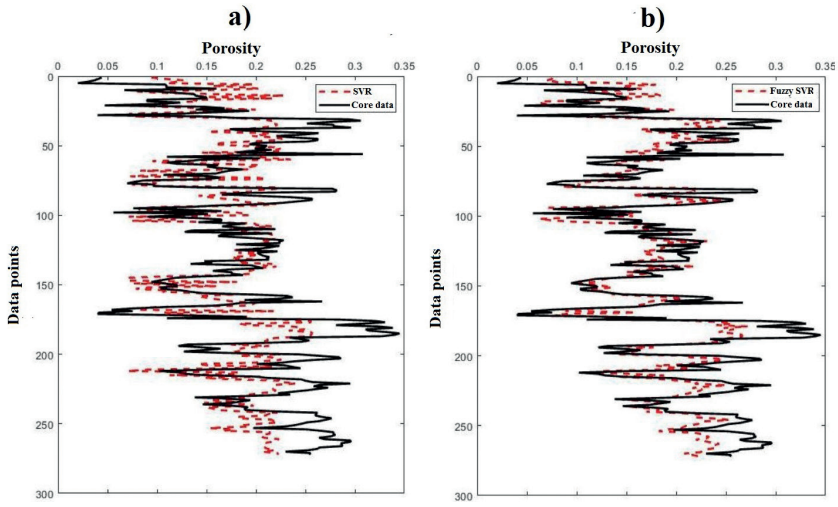

Fig. 11 - Comparison between SVR and fuzzy SVR in the presence of artificial noise in the data: a) the SVR model (red dotted line) and core data (black line); b) the fuzzy SVR model (red dotted line) and core data (black line).

Based on the results in Fig 11. and the calculated *CD*, it is clear how the fuzzy SVR is powerful in the presence of noise in data in comparison to conventional SVR. In this paper, different levels of noise have been added to data. In the presence of a high level of noise in the data, the fuzzy SVR remains robust and the calculated CD does not change very much. Conversely, when the amount of noise in the data increases, the correlation between the SVR prediction result and core data falls dramatically. The main advantage, for this reason, of the fuzzy SVR method is its application for noise suppression in data.

5. Conclusions

In this paper, we utilised SVR to predict a porosity model on real data of an oil field in southern Iran. Initially, the effects of three parameters on the SVR model were investigated. The results

showed how these three parameters can improve or deteriorate the model obtained. Next, we calculated error statistics using different kernels for both SVR and fuzzy SVR, and, then, found the most appropriate kernel for both algorithms. Ultimately, since the presence of noise is inevitable in geophysical data, we modified the SVR to fuzzy SVR by applying membership functions on the data, so that each data point has a contribution on the model by receiving a membership degree. On calculating the *CD* for both fuzzy SVR and SVR versus core data, the results proved that fuzzy SVR is more effective in suppressing the influence of noise on data compared to SVR.

REFERENCES

Al-Anazi A.F. and Gates I.D.; 2012: *Support vector regression to predict porosity and permeability: effect of sample size.* Comput. Geosci., 39, 64-76, doi: 10.1016/j.cageo.2011.06.011.

Bagheri M. and Riahi M.A.; 2015: *Seismic facies analysis from well logs based on supervised classification scheme with different machine learning techniques*. Arabian J. Geosci., 8, 7153-7161, doi: 10.1007/s12517-014-1691-5.

Bagheri M. and Rezaei H.; 2019: *Reservoir rock permeability prediction using SVR based on radial basis function kernel.* Carbonates Evaporites, 34, 699-707.

Bagheri M., Riahi M.A. and Hashemi H.; 2013: *Reservoir lithofacies analysis using 3D seismic in dissimilarity space.* J. Geophys. Eng., 10, 035006, 9 pp., doi: 10.1088/1742-2132/10/3/035006.

Basak D., Pal S. and Patranabis D.C.; 2007: *Support vector regression, neural information processing.* Lett. Rev., 11, 203-224.

Bishop C.M.; 2006: *Pattern recognition and machine learning*. Springer, New York, NY, USA, pp. 325-344.

Blum C. and Roli A.; 2003: *Metaheuristics in combinatorial optimization: overview and conceptual comparison.* ACM Comput. Surv., 35, 268-308, doi: 10.1145/937503.937505.

Esrafili-Dizaji B. and Rahimpour-Bonab H.; 2013: *A review of Permo-Triassic reservoir rocks in the Zagros area, southwest of Iran: influence of the Qatar-Fars arch*. J. Pet. Geol., 36, 257-279.

Gholami R., Shahraki A.R. and Paghaleh M.J.; 2012: *Prediction of hydrocarbon reservoirs permeability using support vector machine.* Math. Prob. Eng., 670723, 18 pp., doi: 10.1155/2012/670723.

Gunn S.R.; 1998: *Support vector machines for classification and regression.* Image Speech and Intelligent Systems Group, University of Southampton, UK, Technical Report, 52 pp.

Hsu C.W., Chang C.C. and Lin C.J.; 2003: *A practical guide to support vector classification.* Department of Computer Science and Information Engineering, National Taiwan University, Taipei, Taiwan, Technical Report, 16 pp.

Huang S., Tian L., Zhang J., Chai X., Wang H. and Zhang H.; 2021: *Support vector regression based on the particle swarm optimization algorithm for tight oil recovery prediction*. ACS Omega, 6, 32142-32150, doi: 10.1021/acsomega.1c04923.

Karimian M., Fathianpou N. and Moghadasi J.; 2013: *The porosity prediction of one of Iran south oil field carbonate reservoirs using support vector regression.* Iran. J. Oil Gas Sci. Tech., 2, 25-36, doi: 10.22050/ijogst.2013.3642.

Keerthi S.S., Sindhwani V. and Chapelle O.; 2007: *An efficient method for gradient based adaptation of hyperparameters in SVM models*. Adv. Neural Inf. Proc. Syst., 19, 673-680, doi: 10.7551/mitpress/7503.003.0089.

Lin C.F. and Wang S.D.; 2002: *Fuzzy support vector machines*. IEEE Trans. Neural Networks, 13, 464-471, doi: 10.1109/72.991432.

Mohamed I.A., Othman A. and Fathy M.; 2020: *A new approach to improve reservoir modeling via machine learning.* The Leading Edge, 39, 170-175, doi: 10.1190/tle39030170.1.

Moosavi N., Bagheri M., Nabi-Bidhendi M. and Heidari R.; 2022: *Fuzzy support vector regression for permeability estimation of petroleum reservoir using well logs.* Acta Geophys., 70, 161-172.

Moosavi N., Bagheri M., Nabi-Bidhendi M. and Heidari R.; 2023a: *Porosity prediction using fuzzy SVR and FCM SVR from well logs of an oil field in south of Iran*. Acta Geophys., 71, 769-782.

Moosavi N., Bagheri M., Nabi-Bidhendi M. and Heidari R.; 2023b: *Prediction of water saturation by FSVM using well logs in a gas field located in south of Iran.* J. Earth Space Phys., 48, 77-86, doi: 10.22059/jesphys.2022.334938.1007389.

Rafik B. and Kamel B.; 2016: *Prediction of permeability and porosity from well log data using the nonparametric regression with multivariate analysis and neural network: Hassi R'Mel Field, Algeria.* Egypt. J. Pet., 26, 763-778.

Rezaee M.R., Kadkhodaei-Ilkhchi A. and Alizadeh P.M.; 2008: *Intelligent approaches for the synthesis of petrophysical logs*. J. Geophys. Eng., 5, 12-26, doi: 10.1088/1742-2132/5/1/002.

Rustam Z., Nurrimah N. and Hidayat R.; 2019: *Indonesia composite index prediction using fuzzy support vector regression with fisher score feature selection*. Int. J. Adv. Sci. Eng. Inf. Tech., 9, 121-128, doi: 10.18517/ijaseit.9.1.8209.

Saputro O., Maulana A. and Latief F.; 2016: *Porosity log prediction using artificial neural network*. J. Phys., Conf. Ser., 739, 012092, 6 pp., doi: 10.1088/1742-6596/739/1/012092.

Sinaga T., Rosid M. and Haidar M.; 2019: *Porosity prediction using neural network based on seismic inversion and seismic attributes.* In: Proc. 4th International Conference on Energy, Environment, Epidemiology and Information System (ICENIS 2019), Semarang, Indonesia, E35 Web Conf., Vol. 125, 15006, 5 pp., doi: 10.1051/e3sconf/201912515006.

Smola J.A. and Scholkopf B.; 1998: *A tutorial on support vector regression*. Stat. Comput., 14, 199-222.

Suykens J.A.K., Van Gestel T., Brabanter J., De Moor B. and Vandewalle J.; 2002*: Least squares support vector machines.* World Scientific, Singapore, 308 pp., doi: 10.1142/5089.

Talbi E-G.; 2009: *Methaheuristics: from design to implementation*. John Wiley & Sons Inc., Hoboken, NJ, USA, 624 pp., doi: 10.1002/9780470496916.

Teixeira A.F. and Secchi A.R.; 2019: *Machine learning models to support reservoir production optimization*. IFAC-PapersOnLine, 52, 498-501, doi: 10.1016/j.ifacol.2019.06.111.

Vapnik V.N.; 1982: *Estimation of dependences based on empirical data.* Springer, New York, NY, USA, 523 pp., doi: 10.1007/0-387-34239-7.

Vapnik V.N.; 1995: *The nature of statistical learning theory*. Springer, New York, NY, USA, 203 pp., doi: 10.1007/978-1-4757-2440-0.

Villmann T., Haase S. and Kaden M.; 2015: *Kernelized vector quantization in gradient-descent learning*. Neurocomput., 147, 83-95.

Wang H. and Xu D.; 2017: *Parameter selection method for support vector regression based on adaptive fusion of the mixed Kernel function*. J. Control Sci. Eng., 2017, 3614790, 12 pp., doi: 10.1155/2017/3614790.

Yin R., Li Q., Li P. and Lu D.; 2020: *A novel method for matching reservoir parameters based on particle swarm optimization and support vector machine*. Math. Prob. Eng., 2020, 7542792, 10 pp., doi: 10.1155/2020/7542792.

Zadeh L.A.; 1965: *Fuzzy sets.* Inf. Control, 8, 338-353.

Corresponding author: Majid Bagheri
Department of Earth Physics, Institute of Geophysics, University of Tehran
North Kargar, Tehran, Iran
Phone: +98 2161118555; e-mail: majidbagheri@ut.ac.ir